TPM Vol. 32, No. S8, 2025
ISSN: 1972-6325
https://www.tpmap.org

RESVERATROL- AND PIPERINE-CO-LOADED NANOSTRUCTURED LIPID CARRIERS FOR INTRANASAL DELIVERY: DEVELOPMENT, CHARACTERIZATION, AND NEUROPROTECTIVE POTENTIAL IN PARKINSON'S DISEASE

NEHA SAINI[1], ABHINAV VERMA[2], TANUSHREE VYAS[2], NEETU PANWAR[3], MADHAV MOHAN[4], RITU KATARIA[5], DIMPY RANI[6*]

[1] g.D. GOENKA UNIVERSITY, SOHNA, GURUGRAM, INDIA (ORCID: 0009-0006-1484-4812)
[2] SCHOOL OF PHARMACY, SHRI VENKATESHWARA UNIVERSITY, GAJRAULA, UP, INDIA (ORCID: 0009-0006-8196-3424)
[2] SCHOOL OF PHARMACY, SHRI VENKATESHWARA UNIVERSITY, GAJRAULA, UP, INDIA (ORCID: 0009-0000-2979-0585)
[3] SCHOOL OF APPLIED SCIENCES, SHRI VENKATESHWARA UNIVERSITY, GAJRAULA, UP, INDIA (ORCID: 0000-0002-2401-7259)
[4] INSTITUTE OF PHARMACY, DOSUT, NALANDA (ORCID: 0009-0004-1347-6435)
[5] GVM COLLEGE OF PHARMACY, SONIPAT, HARYANA, INDIA (ORCID: 0009-0003-3614-9149)
[6] G.D. GOENKA UNIVERSITY, SOHNA, GURUGRAM, INDIA (ORCID: 0000-0003-4618-0177)

GRAPHICAL ABSTRACT

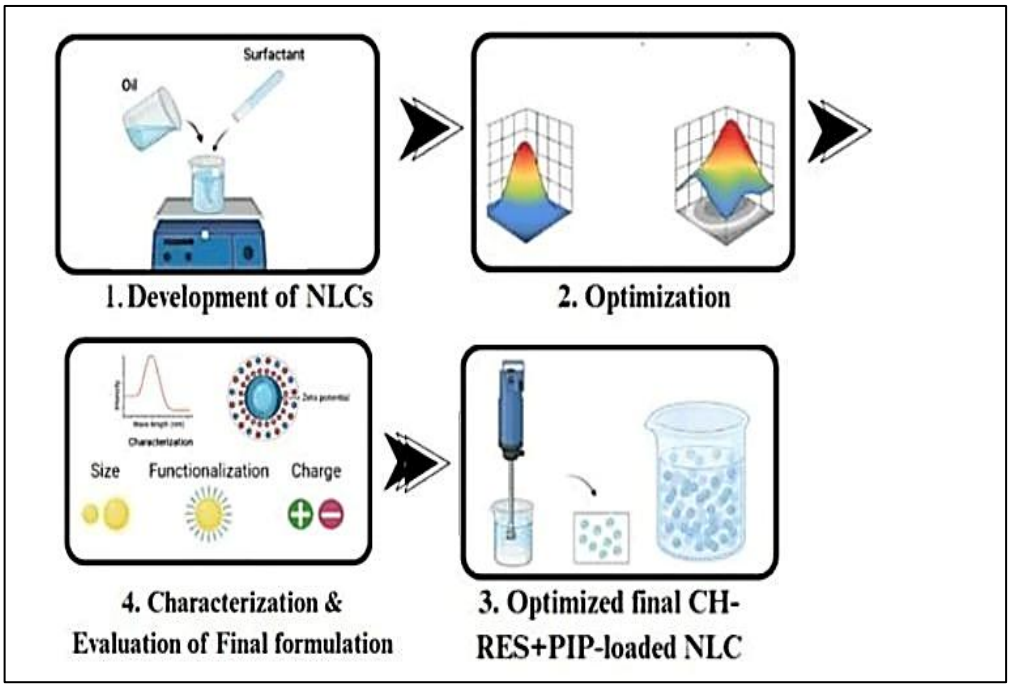

ABSTRACT:

Background: Parkinson's disease (PD) is a progressive neurodegenerative disorder marked by dopaminergic neuronal loss in the substantia nigra and debilitating motor and cognitive impairments. Conventional dopaminergic therapies often show limited brain bioavailability and significant side effects. Naturally occurring compounds such as resveratrol (RES) and piperine (PIP) exhibit potent neuroprotective, antioxidant, and anti-inflammatory activities but suffer from poor solubility and low oral bioavailability, restricting their therapeutic use.

Objective: The present study aimed to develop, characterize, and evaluate chitosan-coated nanostructured lipid carriers (NLCs) co-loaded with RES and PIP for intranasal delivery to achieve improved brain targeting and enhanced neuroprotective efficacy in PD.

Methods: RES- and PIP-loaded NLCs were prepared via high-pressure homogenization and ultrasonication using glyceryl monostearate and medium-chain triglycerides as lipid components. The formulations were optimized using solubility screening and central composite design. Physicochemical characterization included FTIR, dynamic light scattering, zeta potential, DSC, and TEM analyses. Entrapment efficiency, drug loading, pH, and in-vitro diffusion were determined.

TPM Vol. 32, No. S8, 2025
ISSN: 1972-6325
https://www.tpmap.org
Open Access

Results: Optimized NLCs showed a mean particle size of 124.1 nm, zeta potential of +33.9 mV, PDI 0.329, and entrapment efficiency 88%. DSC and FTIR confirmed successful drug encapsulation and physicochemical compatibility. TEM revealed uniform spherical nanoparticles with smooth morphology. In-vitro studies demonstrated sustained and controlled drug release of ~95% over 24 h, with a final pH of 5.6 suitable for nasal administration.
Conclusion: The co-loaded RES-PIP NLCs present a stable, biocompatible, and effective intranasal nanocarrier system capable of bypassing the blood–brain barrier to deliver neuroprotective phytoconstituents directly to the brain.
Keywords: Resveratrol, Piperine, Nanostructured lipid carriers, Intranasal delivery, Parkinson's disease, Neuroprotection, Dopaminergic recovery, Chitosan coating

1. INTRODUCTION

Parkinson's disease (PD) is a neurodegenerative condition that worsens over time and is mainly brought on by a brain dopamine deficit in substantia nigra. Dopaminergic cell death causes a reduction in dopamine, a neurotransmitter involved in mood, movement, muscle control, and memory in the brain of a person with Parkinson's disease[1]. The majority of PD diagnoses are made in elderly patients above the age of 60 years or more, and only 5-10% of cases are thought to be identified before reaching the age of 50[2]. The disease is prevalent due to improper functioning of nigrostriatal pathways, followed by accumulation of cytoplasmic aggregates such as Lewy bodies, filaments, and alpha synuclein [3]. Conventionally prescribed treatments have a majority of the side effects, such as motor difficulties, compulsive disorder, and psychosis with low therapeutic efficacy due to bioavailability concerns. In recent years, phytoconstituents have gained popularity for treating neurological disorders due to their wider therapeutic range and fewer side effects [4].
A number of naturally occurring compounds, such as resveratrol (RES) and piperine (PIP), have garnered interest because of their efficacy and neurological protection. RES (Family: Stilbene) is a naturally occurring polyphenol which is mainly extracted from Veratrum grandiflorum. It has been identified in over 70 plant genera, primarily in the skin and seeds of grapes. It has also been found in trace amounts in red wines and a variety of foods consumed by humans [5]. The two stereo isomeric types of resveratrol that make up its chemical structure are cis-resveratrol and trans-resveratrol[6]. PIP (Family: Piperaceae) is extracted from Piper nigrum & Piper longum which is a nitrogenous compound and belongs to an alkaloidal group. These drugs have been extensively explored across various therapeutic areas because of their complex biological description, which includes neuroprotective, anti-inflammatory, antioxidant, antihypertensive, antitumor, pain reliever, antibacterial, antifungal, hepatoprotective, and antimutagenic[7]. RES & PIP aid in reducing neuroinflammation, oxidative stress, altering the cellular apoptotic, effective against mitochondrial dysfunction and enhancing cognitive abilities in various animal models[8].
Some studies revealed that PIP is used as bioavailability enhancer by inhibiting the enzymes, required to metabolize the drugs. Shoba et al., suggested that PIP influences the pharmacokinetic properties of curcumin in animal models as well as human volunteers[9]. Another research demonstrated that combining resveratrol with piperine significantly enhances the bioavailability and pharmacokinetic parameters of resveratrol by constraining its glucuronidation, thereby minimizing its elimination. However, it requires more in-depth investigation to determine the effects on metabolic pathways and bioavailability of resveratrol by combining it with piperine[10]. Despite having poor aqueous solubility and bioabsorption, these phytoconstituents have been extensively researched due to their numerous benefits in treating brain diseases. Nevertheless, categorised in BCS class II, which has low bioavailability and solubility problems that restrict its targets to the site of action and limit its potential for clinical development. Therefore, the use of sophisticated preparation and nanotechnology-based methods has been developed to get around these problems and stimulate its pharmacological action[8]. Nanostructured lipid carriers are considered a promising approach to quickly transport medications directly to the brain through nasal mucosa with increased bioavailability of drug. The nose-to-brain route is considered safer and non-invasive route to attain effective therapeutic action with fewer side effects[11-13].
Previously, Zafar et al., formulated a chitosan coated piperine NLCs via oral route for the diabetic disease[14]. Yadav et al., reported a piperine loaded mucoadhesive nano-emulsion by titration method for nasal route to enhance its in vivo bioavailability[15]. Elnaggar et al., formulated chitosan nanoparticles with piperine for targeting Alzheimer's disease through intranasal delivery[16]. Bahareh et al., designed resveratrol loaded nanocarriers (NLCs) for the management of skin cancer. Furthermore, aspects like in vivo testing, stability studies and clinical efficacy and safety were not discussed thoroughly[17]. A study reported by whitehead et al., focused on resveratrol loaded NLCs, fabricated to investigate the Vaso-protective as well as antioxidant effects[18]. Kumar et al., formulated a resveratrol nanocarrier (NLCs) for treating Glioblastoma Multiforme via nose to brain route[19]. Jadhav et al., prepared mixed micelles by combining RES and PIP. Despite these, the most challenging is the scaleup process with precise lipid composition leads to stability of the formulation.[20] However, these studies needed the proper discussion pattern of stability studies, clinical efficacy, optimization pattern and characterization of the developed formulation with ex vivo and in vivo studies. Though these problems can be avoided by incorporating the drugs (RES & PIP) into a suitable nanocarrier such as NLC, which can be proven as an advantageous nano-system by masking the associated limitations of drugs and influencing the drug delivery through the nasal route.[21]
This research is based on the controlled release approach of NLCs loaded with chitosan coated RES combined PIP for its targeted delivery in brain for neuroprotective effects.

2. MATERIALS AND METHODS

2.1. Materials:

RES (B.No. RHMPL/15082022/5790) and PIP (B.No. RHMPL/222222/5790) were purchased from Reeyansh Herb Mantra Pvt. Ltd., India. Chitosan and Glyceryl monostearate were obtained from Loba Chemie Pvt. Ltd. PVA (Polyvinyl alcohol) and Tween 80 were purchased from Nice Chemicals (P) Ltd. Medium chain triglycerides (Nutiva MCT oil) was purchased from Indian e-commerce site Amazon. All the chemicals used were of analytical grade.

2.2. Methods:

2.2.1. Optimization

The selection of lipids was done by solubility studies. The solution of lipids (glyceryl monostearate, stearic acid, compritol 888 ATO, precirol ATO 5) was prepared by dissolving each solid lipid (1g) in ethanol (10ml) and heating at 50-60^{0}C on water bath to ensure complete mixing. In the mixtures, an excess amount of drugs (10mg) was added, vortexed for 5 minutes, and then subjected to ultrasonication for 10 minutes at 40kHz, incubated at 37 ^{0}C for 24 hours. Centrifuged the mixtures at 10,000 rpm for 15 minutes to separate the undissolved drug from the supernatant. The drug concentrations (diluent: ethanol) were measured using UV-Vis spectrophotometer (Shimadzu UV-1900) at 306 nm for RES and 342 nm for PIP. The solubility (mg/ml) was calculated using the following formula:

Solubility (mg/ml) = Concentration of drug in supernatant (mg)/Volume of solvent (ml)

2.2.2. Development of RES and PIP based NLCs

The drugs loaded NLCs were prepared by high high-pressure homogenization method followed by ultrasonication as reported earlier [22,23,24] Briefly, Glyceryl monostearate (GMS, solid lipid) and MCT oil (Liquid lipid) were melted at 70°C which was 5°C above the melting point of solid lipid. Then the drug, RES (API) and PIP (API) in desired amount (50mg) was dissolved in the melted lipid phase to ensure even dispersion of the drugs. Now, separately aqueous solution was prepared by dissolving Tween 80 (surfactant) in distilled water and heated at 70°C. Lipid phase was added to the aqueous phase dropwise with constant stirring using a high shear homogenizer (IKA T25, Ultra Turrax, Germany) to form the coarse emulsion. The mixture was then subjected to ultrasonication (Pricisonic USB6.5L) for 5 minutes to reduce the particle size of emulsion droplets. The emulsion was cooled rapidly to solidify the lipid which formed NLCs. Chitosan (mucoadhesive agent) solution (1-2%w/v) was also added to the dispersion under stirring to coat the NLCs.

2.3. CHARACTERIZATION:

2.3.1. FTIR

FTIR (SPIRIT-X) was done using QATR-S with lab solution lite software (ver. 1.122 & 2.33) sample compartment and analysis was performed by transmission. The standard KBr disc method was employed in which sample/KBr (1/100) ratio was used to create pellets enclosing samples gently with anhydrous KBr. The spectrum was obtained between 500-4000 cm^{-1}.

2.3.2. Particle size and Zeta potential

The mean particle size and zeta potential of NLCs were analysed by dynamic light scattering (DLS) instrument (Malvern, Zetasizer). NLC suspension was diluted with distilled water to an appropriate concentration and filtered through a 0.22 µm filter to remove any large particles or aggregates. The filtered sample was transferred into a cuvette to measure the particle size distribution and zeta potential of the NLCs. The instrument software (Malvern 2.0) calculated the average particle size (Z-average) and polydispersity index (PDI) from the light scattering data [25].

2.3.3. Calorimetric Analysis

Placed an accurately weighed samples (5mg) in a standard aluminium DSC pan. The pan was sealed using crimper to prevent any loss of sample during the heating process. The melting point, thermal decomposition and glass transition state of formulation (NLC) thermograms were recorded from 30°C to 250°C by calibrated differential scanning calorimetry (Shimadzu 13.1 software). The analysis was done under a nitrogen atmosphere at a flow rate of 50 mL/min to prevent oxidation and ensure an inert environment.

2.3.4. TEM (transmission electron microscopy)

The morphology of drug-loaded NLCs was discerned by TEM (transmission electron microscopy, water 2.0 software). The samples were prepared by adding a small amount of NLCs into deionized water (5ml) then a droplet was added on the paraffin sheet followed by positioning a carbon-coated grid on sample. The grid was left undisturbed for 1min to enable the combined NLCs to stick to the carbon substrate. The excess of sample was carefully removed by using edge of filter paper. The samples were air-dried without staining before examination [26].

2.4. EVALUATION PARAMETERS:

2.4.1. Entrapment Efficiency and Drug Loading

It determines the percentage of drug entrapped into the NLC particles and the free drug remaining in the NLC suspension. NLC suspension was centrifuged (20,000 rpm) to separate the free drug from the encapsulated drug. The supernatant containing free drug was carefully collected and analyzed using UV-Vis spectroscopy (Shimadzu UV-1900). The entrapment efficiency and concentration of free drug (drug loading) were determined using the given formula [27]:

EE (%) = Total drug – Free drug/ Total drug x 100

DL (%) = Total drug- Free drug/ Weight of NLC x 100.

2.4.2. In-vitro diffusion studies

Placed an appropriate amount of NLC suspension into a dialysis bag and sealed it securely. A suitable release medium (phosphate-buffered saline PBS, pH 7.4) used with temperature maintaining at 37°C throughout the experiment. Dialysis bag was placed in the dissolution medium and started the apparatus (USP Type II) at constant speed 100 rpm. The samples

were withdrawn (5ml) at predetermined time intervals (0,0.5,1,2,3,4,5,6,8,12,24 hours) and replaced the withdrawn samples with fresh medium. Analyze the amount of drug released using UV-Vis spectroscopy (Shimadzu UV-1900)[28].

2.4.3. pH

The pH of the nasal formulation should be within the physiologically acceptable range of 5.5 to 6.5 to ensure compatibility with the nasal mucosa and prevent irritation. The pH was measured by digital pH meter (Eutech Instruments, Model: 700).

3. RESULTS AND DISCUSSION:

3.1. Optimization

Based on the experimental data, RES has the highest solubility 4.0mg/ml in Compritol 888 ATO (solid lipid) while PIP has the highest solubility 4.0mg/ml in Glyceryl Monostearate (solid lipid). For liquid lipids, both RES 6.0mg/ml and PIP 6.5mg/ml show the highest solubility in Caprylic/Capric Triglycerides (MCT Oil). Particle Size decreases with increasing homogenization speed and lipid concentration. Entrapment Efficiency increases with optimized lipid concentration and sonication time, indicating that higher levels of both RES and PIP were encapsulated within the lipid carriers. The 3D surface plot for combined RES & PIP loaded NLCs are shown in figure 1.

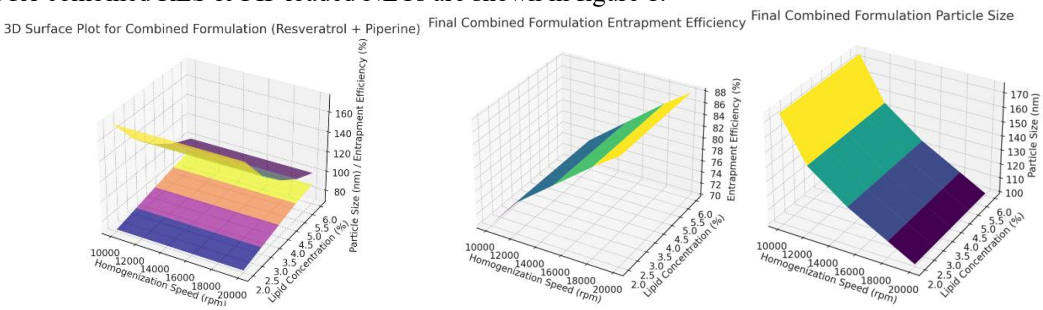

Figure 1: 3 D surface plots for combined formulation by using Central composite design

3.2. Characterization

3.2.1. FTIR studies

The peaks in between ~1600-1580 cm^-1 indicates the presence of aromatic C=C bonds stretching and ~3300-3400 cm^-1 corresponds to N-H stretching vibration which confirm the functional groups present in PIP. The FTIR absorption peak between ~1250-1000 cm^-1 represented C-O-C stretching from methylenedioxy group. Peak around 2900 cm^-1 presented C-H stretch from aliphatic chains and sharp peak around ~1650 cm^-1 showed C=O stretch for amides[46]. The peaks confirm the functional groups present in RES at ~3300 cm^{-1} represented bending vibration of O-H Stretching, Aromatic C=C Stretching (1600-1510 cm^{-1}), ~970 cm^{-1} C=C configuration for stilbene and C-O Stretching (1250-1020 cm^{-1}). The graph of combined NLC (Fig. 2) shows combined peaks of RES and PIP, with possible additional peaks due to the excipient[47].

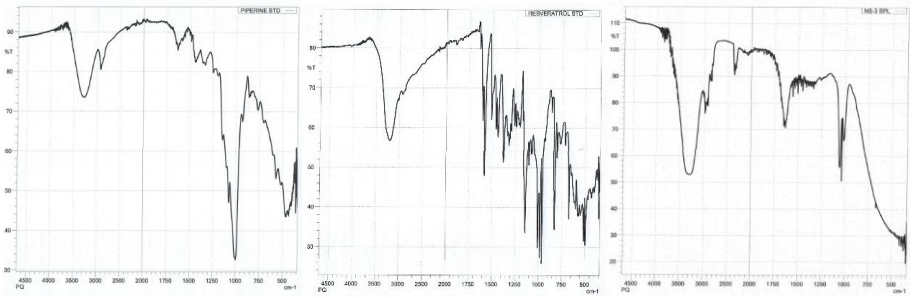

Figure 2: FTIR graphs of pure PIP, RES and Final combined NLC formulation

3.2.2. Particle size, zeta potential & PDI

Particle sizes decrease from 185 nm to 145 nm in batches taken for optimization, all below 200 nm, which is ideal for efficient drug delivery, particularly via the intranasal route. The Zeta Potential values range from +21.0 mV to +33.0 mV in among trial batches. According to prior research or theory of DLVO (Derjaguine Landaue Verweye Overbeek), zeta potential higher than +30.00 and −30.00 mV are more stable.[48] The highest positive charge of combined RES and PIP loaded NLC (33.9mV) suggested that the formulation possess good stability. The PDI decreases from 0.42 to 0.35 in batches. A lower PDI indicates a more uniform particle size distribution, which is desirable for consistent drug delivery. The final optimized batch has resulted 124.1 nm average size with PDI (0.329) as represented in figure 3.

Figure 3: Graph shows the size distribution and Zeta potential across the optimized batches.

3.2.3. DSC

The broad peak in DSC thermogram (fig. 4) confirmed successful encapsulation within the NLC. The thermal shifts indicated strong interactions between the drugs and the lipid matrix, enhancing drug loading and controlled release. This interaction also enhances the thermal stability of the formulation by supporting drugs incorporation with potential molecular-level interactions. This thermal behavior suggested that the NLC formulation will enhance the bioavailability and drug dissolution and making it as an effective nanocarrier for sustained drug delivery.

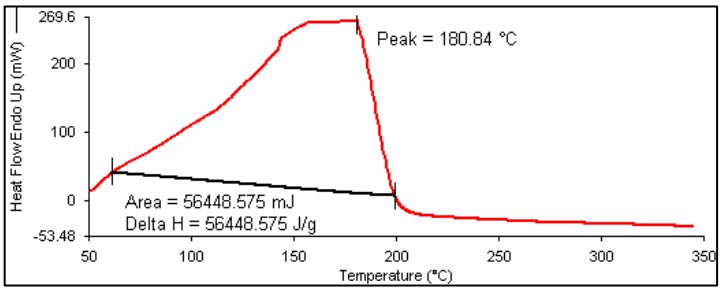

Figure 4: DSC thermogram of combined NLCs

3.2.4. TEM

The TEM images at 200 nm scale (figure 5) has shown near-spherical NLCs particles with smooth surface and consistent particle size without any significant aggregation, confirming the success of the formulation with stable and effective delivery system.

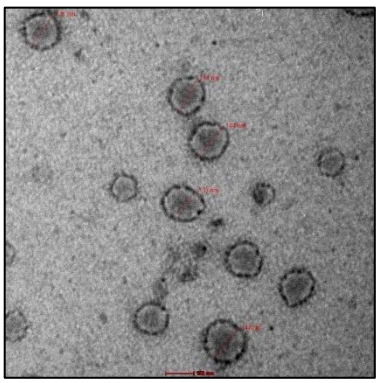

Figure 5: TEM image of Combined (RES and PIP) NLCs

3.3. Evaluation Parameters:

3.3.1. Entrapment Efficiency & Drug Loading (%)

Entrapment Efficiency increases from 78% to 88% in trial batches. Higher entrapment efficiency ensures that a greater amount of the active drugs (RES and PIP) is encapsulated within the NLCs, enhancing the formulation's therapeutic potential. Drug Loading increases from 5.5% to 7.0% among different batches, indicating that the formulation can carry a higher amount of the active drugs within the NLCs without compromising stability or performance.

3.3.2. In-Vitro Cumulative Release (%)

The In-Vitro Cumulative Release improves from 65% to 82% in trial batches, indicating a more controlled and sustained release profile which is crucial for maintaining therapeutic levels of the drugs over an extended period. The final optimized batch has shown 95% drug release in 24 hours (as highlighted in figure 6) indicating more efficient formulation in encapsulating and releasing the drugs.

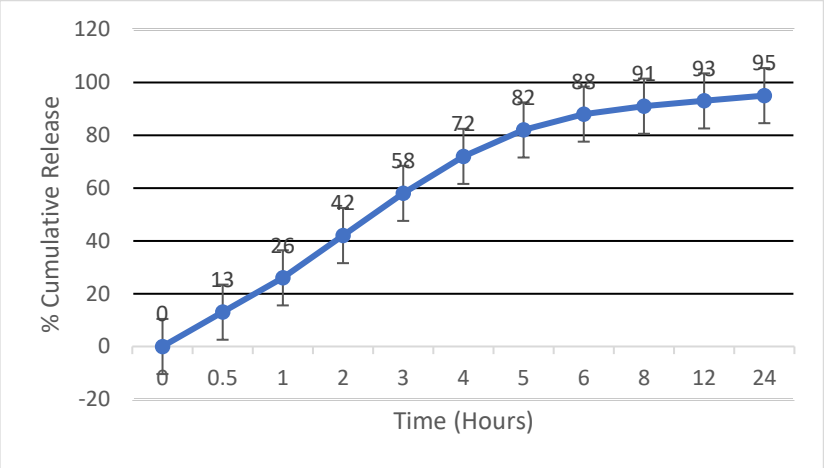

Figure 6: Graph showing correlation between entrapment efficiency and in-vitro cumulative release for combined NLCs

3.3.3. pH

The formulation containing RES and PIP is weakly acidic and needs pH adjustment to achieve within range. So initially the pH of the developed nasal formulation was measured to be 4.1 which was adjusted by incrementally adding approximately 1.8 mL of 0.1 M NaOH. After addition, the final pH of the formulation stabilized at 5.6 after 2 hours, confirming the robustness of the adjustment process.

DISCUSSION

The solubility studies showed that the selection of lipids for NLC preparation was ideal with higher solubility of drugs in the lipid matrix, confirming their suitability for integration into lipid base. Enhanced solubility in these lipids indicated a higher potential for effective drug encapsulation, ensuring improved bioavailability through lipid-based drug delivery.
The FTIR spectrum confirm that RES and PIP were successfully incorporated into NLC. In addition to characteristic peaks of both drugs, new peaks are also present indicating the interactions between the drugs and excipients. It further suggests that the absence of significant shifts in functional groups indicating chemical integrity of both drugs in the formulation which is also necessary to maintain their therapeutic efficacy. The particles sizes were optimized among the batches from 185nm to 145nm with a decrease in PDI from 0.42 to 0.35 which signifies a uniform stable dispersion for nasal delivery and efficiently penetrate through BBB to reach the site of action. The zeta potential indicated a stable colloidal system by reducing the risks of aggregation of particles which directly enhances the stability of NLCs. The high drug loading and encapsulation efficiency reflects the maximizing therapeutic effects of the drugs in the brain. This implies that the brain can receive adequate drug concentrations from the optimised batch, lowering the frequency of doses and increasing patient compliance.
An increased cumulative drug release among different batches suggested sustained & controlled release from NLCs which enhances neuroprotection, reducing side effects, and maintaining consistent therapeutic levels. The DSC graph reveal substantial improvements in thermal stability of both drugs upon encapsulation. The changes in peak and onset temperatures show the way drugs interact with the lipid matrix, which improves the stability of the drugs and decreases their crystallinity. This thermal behaviour is essential for maintaining controlled release by avoiding degradation of drug and also ensures long term stability of formulated nanocarriers. The pH of the formulation was initially adjusted from 4.1 to 5.6, which enhances the compatibility of nasal membrane while reducing the chances of irritation. The isotonicity of the final formulation delivered through nasal route was maintained by adding NaCl which further improves the patient tolerability by reducing osmotic stress on nasal tissues. These modifications enhance the viability of long-term intranasal administration. The morphology of NLCs confirms the spherical shape with smooth surfaces, uniform size and minimal aggregation which is ideal for intranasal delivery and also allows particles to cross BBB easily.

CONCLUSION:

The research highlights an effective approach to develop a combined NLCs formulation of RES and PIP for the intranasal administration, providing increased bioavailability, controlled drug release and improved stability. This formulation holds an enormous potential for managing neurodegenerative diseases like Parkinson's disease, leveraging nanotechnology to circumvent within the constraints of conventional drug delivery. Future research should concentrate on long-term stability and large-scale manufacturing challenges to promote clinical translation.

REFERENCES:

1. Emamzadeh, F.; Surguchov, A. Parkinson's disease : Biomarkers, Treatment, and Risk Factors. Front. Neurosci., **2018**, 12, 612. https://doi.org/10.3389/fnins.2018.00612

2. https://www.ninds.nih.gov/current-research/focus-disorders/parkinsons-disease-research/parkinsons-disease-challenges-progress-and-promise
3. Dickson, D.W. Parkinson's Disease and Parkinsonism: Neuropathology. Cold Spring Harb. Perspect. Med. 2012, 2, a009258. http://perspectivesinmedicine.cshlp.org/
4. Qizilbash, F..F.; Ashhar, M.U.; Zafar, A.; Qamar, Z.; Ali, A.J.; Baboota, S.; Ghoneim, M.M.; Alshehri, S.; Ali, A. Thymoquinone-Enriched Naringenin-Loaded Nanostructured Lipid Carrier for Brain Delivery via Nasal Route: In Vitro Prospect and In Vivo Therapeutic Efficacy for the Treatment of Depression. Pharmaceutics, **2022**, 14, 656. https://doi.org/10.3390/pharmaceutics14030656
5. Salehi, B.; Mishra, A.P.; Nigam, M.; Sener, B.; Kilic, M.; Sharifi-Rad, M.; Fokou, P.V.T.; Martins, N.; Sharifi-Rad, J. Resveratrol: A Double-Edged Sword in Health Benefits. Biomedicines. **2018**, 6(3):91. doi: 10.3390/biomedicines6030091.
6. Carlotti, M.E.;, Sapino, S.; Ugazio, E.; Gallarate, M.; Morel, S. Resveratrol in Solid Lipid Nanoparticles. Journal of Dispersion Science and Technology, **2012** 33:4, 465-471, DOI:10.1080/01932691.2010.548274
7. Gupta I, Adin SN, Aqil M, Mujeeb M, Ahad A. Computer-aided Box–Behnken outlook towards optimization of extraction of piperine from Piper longum L. Fruits. World J Pharm Res. **2022** 11, 1439-55.
8. Neuroprotective Potential of Silymarin against CNS Disorders: Insight into the Pathways and Molecular Mechanisms of Action. CNS Neurosci. Ther. **2013**, 19, 847.
9. Raza, S.S.; Khan, M.M.; Ashafaq, M.; Ahmad, A.; Khuwaja, G.; Khan, A.; Siddiqui, M.S.; Safhi, M.M.; Islam, F. Silymarin Protects Neurons from Oxidative Stress Associated Damages in Focal Cerebral Ischemia: A Behavioral, Biochemical and Immunohistological Study in Wistar Rats. J. Neurol. Sci. **2011**, 309, 45–54.
10. Zhang, L.-X.; Li, C.-X.; Kakar, M. U.; Khan, M.S.; Wu, P.-F.; Amir, R. M.; Dai, D.-F.; Naveed, M.; Li, Q.-Y.; S, M.; Shen, J.-Q.; Rajput, S.A.; Li, J.-H. Resveratrol (RV): A pharmacological review and call for further research. Biomedicine & Pharmacotherapy. **2021**, 143, 112164. https://doi.org/10.1016/j.biopha.2021.112164
11. Fan, P.; Marston, A.; Hay, A.-E.; Hostettmann, K. Rapid separation of three glucosylated resveratrol analogues from the invasive plant Polygonum cuspidatum by high-speed countercurrent chromatography. J. Sep. Sci. **2009**, 32:2979–2984. doi: 10.1002/jssc.200900057
12. Duarte, A.; Martinho, A.; Luís, Â.; Figueiras, A.; Oleastro, M.; Domingues, F.C.; Silva, F. Resveratrol encapsulation with methyl-β-cyclodextrin for antibacterial and antioxidant delivery applications. Food Sci. Technol. **2015**, 63:1254–1260. doi: 10.1016/j.lwt.2015.04.004
13. Zhang, L.-X.; Li, C.-X.; Kakar, M.U.; Khan, M.S.; Wu, P.-F.; Amir, R.M.; Dai, D.-F.; Naveed, M.; Li, Q.-Y.; Saeed, M.; Shen, J.-Q.; Rajput, S.A.; Li, J.-H. Resveratrol (RV): A pharmacological review and call for further research. Biomedicine & Pharmacotherapy. **2021**, 143, 112164, ISSN 0753-3322, https://doi.org/10.1016/j.biopha.2021.112164.
14. Shoba, G.; Joy, D.; Joseph, T.; Majeed, M.; Rajendran, R.; Srinivas, P.S. Influence of piperine on the pharmacokinetics of curcumin in animals and human volunteers. Planta Med. **1998,** 64(4), 353-6. doi: 10.1055/s-2006-957450.
15. Johnson, J.J.; Nihal, M.; Siddiqui, I.A.; Scarlett, C.O.; Bailey, H.H.; Mukhtar, H.; Ahmad, N. Enhancing the bioavailability of resveratrol by combining it with piperine. Mol Nutr Food Res. **2011,** 55(8):1169-76. doi: 10.1002/mnfr.201100117.
16. Elnaggar, Y.S.R.; Etman, S.M.; Abdelmonsif, D.A.; Abdallah, O.Y. Intranasal Piperine-Loaded Chitosan Nanoparticles as Brain-Targeted Therapy in Alzheimer's Disease: Optimization, Biological Efficacy, and Potential Toxicity. Journal of Pharmaceutical sciences, **2015,** 104 (10). 10.1002/jps.24557
17. Bahareh, T.; Ramin, S.; Hossein, S. Development and in vitro evaluation of resveratrol-loaded NLCs for skin cancer treatment. Drug Delivery, **2015**, 22(1), 84-91.
18. Astley, C.; Houacine, C.; Zaabalawi, A.; Wilkinson, F.; Lightfoot, A.P.; Alexander, Y.; Whitehead, D.; Singh, K.K.; Azzawi, M. Nanostructured Lipid Carriers Deliver Resveratrol, Restoring Attenuated Dilation in Small Coronary Arteries, via the AMPK Pathway. Biomedicines **2021**, 9, 1852. https://doi.org/10.3390/biomedicines9121852
19. Kumar, N.; Gupta, G.D.; Arora, D.DoE Directed Optimization, Development and Characterization of Resveratrol Loaded Nlc System for the Nose to Brain Delivery in the Management of Glioblastoma Multiforme. 08 June 2021, PREPRINT (Version 1) available at Research Square [https://doi.org/10.21203/rs.3.rs-572155/v1]
20. Jadhav, P.; Bothiraja, C.; Pawar, A. Resveratrol-piperine loaded mixed micelles: formulation, characterization, bioavailability, safety and in vitro anticancer activity. RSC Adv., **2016**,6, 112795-112805. https://doi.org/10.1039/C6RA24595A
21. Elmowafy, M.; Al-Sanea, M.M. Nanostructured lipid carriers (NLCs) as drug delivery platform: Advances in formulation and delivery strategies. Saudi Pharm J. **2021,** 29(9), 999-1012. 10.1016/j.jsps.2021.07.015.
22. Zardini, A. A.; Mohebbi, M.; Farhoosh, R.; Bolurian, S. Production and characterization of nanostructured lipid carriers and solid lipid nanoparticles containing lycopene for food fortification. J Food Sci Techno, **2018**, 55, 287–298. https://doi.org/10.1007/s13197-017-2937-5
23. Weber, S.; Zimmer, A.; Paradeike, J. Solid lipid nanoparticle (SLN) and Nanostructured Lipid Carriers (NLC) for pulmonary application: A review of the state of the art. European Journal of Pharmaceutics and Biopharmaceutics,**2014,** 86(1), 7-22. https://doi.org/10.1016/j.ejpb.2013.08.013
24. Abo El-Enin, H.A.; Elkomy, M.H.; Naguib, I.A.; Ahmed, M.F.; Alsaidan, O.A.; Alsalahat, I.; Ghoneim, M.M.; Eid, H.M.;. Lipid Nanocarriers Overlaid with Chitosan for Brain Delivery of Berberine via the Nasal Route. Pharmaceuticals (Basel), **2022**;15(3):281. doi:10.3390/ph15030281

25. Bhattacharjee, S. DLS and zeta potential – What they are and what they are not? Journal of Controlled Release, **2016**, 235, 337-351. DOI: 10.1016/j.jconrel.2016.06.017
26. Fazil, M.; Md, S.; Haque, S.; Kumar, M.; Baboota, S.; Sahni, J. K.; & Ali, J. Development and evaluation of rivastigmine loaded chitosan nanoparticles for brain targeting. Eur J Pharm Sci. **2012**, 47, 1, 6-15. doi:10.1016/j.ejps.2012.04.013
27. Puglia, C.; & Bonina, F. Lipid nanoparticles as novel delivery systems for drugs. Future Science, **2006**, 3(5), 637-650. DOI: 10.1517/17425247.2012.666967
28. Zeng, X.; & Gao, C. Controlled Release Systems for Intranasal Drug Delivery. In Nanotechnology in Drug Delivery, **2015**, 111-139. CRC Press.
29. Kilkenny, C.; Browne, W. J.; Cuthill, I. C.; Emerson, M.; & Altman, D. G. Improving bioscience research reporting: The ARRIVE guidelines for reporting animal research. PLoS Biology. **2010**, 8, 6, e1000412. https://doi.org/10.1371/journal.pbio.1000412
30. Santiago, M.; Alcalde, V.; Granero, L.; Felipo, V. Use of 6-OHDA lesion rat model to evaluate new therapeutic strategies for Parkinson's disease. European Journal of Neuroscience. **2010,** 32, 2, 208–219.
31. https://doi.org/10.1111/j.1460-9568.2010.07272.x
32. Paxinos, G., & Watson, C. The rat brain in stereotaxic coordinates (6th ed.). Academic Press. **2007.**
33. Priprem, A.; Chonpathompikunlert, P.; Sutthiparinyanont, S.; Wattanathorn, J. Antidepressant and cognitive activities of intranasal piperine-encapsulated liposomes. Adv Biosci Biotechnol. **2011,** 2, 02, 108–116.
34. DOI:10.4236/abb.2011.22017
35. Mallet, N., Ballion, B., Moine, C. L., & Gonon, F. Rotarod test for measuring motor coordination in rats with nigrostriatal lesions. Journal of Neuroscience Methods. **2012**, 199, 2, 215–222.
36. https://doi.org/10.1016/j.jneumeth.2011.06.022
37. Prut, L., & Belzung, C. The open field as a paradigm to measure the effects of drugs on anxiety-like behaviors: A review. European Journal of Pharmacology. **2003**, 463, 1–3, 3–33. https://doi.org/10.1016/S0014-2999(03)01243-2
38. Tarantino, L. M., Sullivan, P., & Hannon, R. M. Measuring behavior and locomotor activity in rodents. Current Protocols in Neuroscience. **2016**, 77(1), 8-23. https://doi.org/10.1002/cpns.101
39. Hughes, R. N. The value of spontaneous alternation behavior (SAB) as a test of retention in pharmacological investigations of memory. Neuroscience & Biobehavioral Reviews. **2004**, 28, 5, 497–505. https://doi.org/10.1016/j.neubiorev.2004.06.006
40. Vorhees, C. V., & Williams, M. T. Morris Water Maze: Procedures for assessing spatial and related forms of learning and memory. Nature Protocols. 2006, 1, 2, 848–858. https://doi.org/10.1038/nprot.2006.116
41. He, J., Yang, H., Wei, H., & Zhao, Z. Dopamine determination using HPLC with electrochemical detection. Analytical Chemistry. **2020**, 92, 7, 5293–5299. https://doi.org/10.1021/acs.analchem.9b04847
42. Patel, A. B., Lai, J. C. K., & Mehta, P. K. GABA quantification in brain tissues using HPLC. Brain Research Protocols. **2021**, 24, 3, 123–132. https://doi.org/10.1016/j.brainres.2021.118501
43. Ohkawa, H., Ohishi, N., & Yagi, K. Assay for lipid peroxides in animal tissues by thiobarbituric acid reaction. Analytical Biochemistry. **1979**, 95, 2, 351–358. https://doi.org/10.1016/0003-2697(79)90738-3
44. Marklund, S., & Marklund, G. Involvement of the superoxide anion radical in the autoxidation of pyrogallol and a convenient assay for superoxide dismutase. European Journal of Biochemistry. **1974**, 47, 3, 469–474. https://doi.org/10.1111/j.1432-1033.1974.tb03714.x
45. Ellman, G. L. Tissue sulfhydryl groups. Archives of Biochemistry and Biophysics, **1959**, 82, 1, 70–77. https://doi.org/10.1016/0003-9861(59)90090-6
46. Aebi, H. Catalase in vitro. Methods in Enzymology. **1984**, 105, 121–126. https://doi.org/10.1016/S0076-6879(84)05016-3
47. Kiernan, J. A. Histological and histochemical methods: Theory and practice. Scion Publishing Ltd. **2015,** 5th edition, 571pp.
48. Fischer, A. H., Jacobson, K. A., Rose, J., & Zeller, R. Hematoxylin and eosin staining of tissue and cell sections. Cold Spring Harbor Protocols. **2008,** 5, pdb.prot4986. https://doi.org/10.1101/pdb.prot4986
49. Listantia, N.; Bayani, F. Isolation and Characterization of the bioactive compound of piperine in Black Pepper (Piper nigrum L.). Prisma Sains : Jurnal Pengkajian Ilmu dan Pembelajaran Matematika dan IPA IKIP Mataram. **2021,** 9(2), 396-401. doi:https://doi.org/10.33394/j-ps.v9i2.4608
50. Sun, J.; Zhou, Y.; Su, Y.; Li, S.; Dong, J.; He, Q.; Cao, Y.; Lu, T.; Qin, L. Resveratrol-Loaded Solid Lipid Nanoparticle Supplementation Ameliorates Physical Fatigue by Improving Mitochondrial Quality Control. Crystals **2019**, 9, 559. https://doi.org/10.3390/cryst9110559
51. Rasmussen, M.K.; Pedersen, J.N.; Marie, R. Size and surface charge characterization of nanoparticles with a salt gradient. Nat Commun. **2020**, 11, 2337. https://doi.org/10.1038/s41467-020-15889-3